INTELLIGENT IMAGE PROSPECTING SYSTEM FOR IMAGE/RPI MISSION

Ivan A. GALKIN, Center for Atmospheric Research, University of Massachusetts Lowell, USA, Ivan_Galkin@uml.edu
Grigori M. KHMYROV, Center for Atmospheric Research, University of Massachusetts Lowell, USA, Grigori_Khmyrov@uml.edu
Alexander V. KOZLOV, Center for Atmospheric Research, University of Massachusetts Lowell, USA, Alexandre_Kozlov@uml.edu
Bodo W. REINISCH, Center for Atmospheric Research, University of Massachusetts Lowell, USA, Bodo_Reinisch@uml.edu
Shing F. FUNG, NASA Goddard Space Flight Center, USA, Shing.F.Fung@nasa.gov

ABSTRACT

The Radio Plasma Imager (RPI) onboard NASA's IMAGE spacecraft has acquired over 1.2 million *plasmagrams*, images of remote sensing of the Earth's magnetosphere. Plasmagram archive is a classic-example dataset posing unrealistic demands of manual labor in order to analyze each collected image for useful features. We present an intelligent data prospecting system based on a bio-plausible model of the pre-attentive vision whose purpose is to draw attention of human analysts to the most interesting data. Presence of weak signatures in the RPI plasmagrams makes this dataset an excellent testbed for sensitive image prospecting techniques. We discuss our progress to date.

KEYWORDS: Intelligent Systems, Data Prospecting, Pre-attentive Vision Models, Radio Plasma Imager

1. INTRODUCTION

An increasing number of video/image capturing applications rely on intelligent systems for imagery data prospecting in order to cope with the visual information avalanche. Intelligent prospecting is about finding meaningful data among data that just takes up space and then drawing attention of the human analysts to found nuggets.

Our study was originally inspired by the need of getting an insight into the depths of the NASA data archive holding 1.2 million of plasmagram images acquired by the Radio Plasma Imager (RPI) [1] onboard the IMAGE spacecraft [2]. Many other Earth and space physics projects operate under similar pressure of the sheer volume of collected data (e.g., IVOA alliance virtual astronomical observatories, EOSDIS Earth observing sensor network, etc.). Other application domains for image prospecting include unmanned real-time warning systems, autonomous explorers such as the Mars rover, systems for knowledge discovery, etc.

Building an imagery data prospector is a significant task that involves modeling of the visual data perception by humans. Such model commonly includes a feature binding algorithm tailored to the specifics of the domain. Robustness of the feature binding approach to various real-life imperfections of the images is the key to successful solution of the prospecting task.

2. PRE-ATTENTIVE VISION AND DATA PROSPECTING

Biologically plausible models of visual data perception recently are drawing much attention for their potential in replicating the most sophisticated, adaptive, robust, and intelligent image analysis system that we know of. Of particular interest to data prospecting are models of the so-called "pre-attentive" vision system that is found in many living organisms. The pre-attentive vision is a perceptual system whose responsibility is to "pop-up" cues in the field of view without

willful concentration of attention. It is especially effective in rapid detection of salient objects by identifying their contours.

Existing studies of the pre-attentive vision suggest that it adheres to a "bottom-up" analysis strategy that assumes no prior knowledge of the features to be discovered in the analyzed image and relies only on a general perceptual quality of the image features that makes them stand out against the background. Classic bottom-up feature extraction algorithms [4]-[12] first seek detectable low-level image features (dots, bars) that can be grouped together in salient contours under Gestalt restrictions [3] of proximity, good continuation, and smoothness.

3. RADIO PLASMA IMAGER DATASET

The RPI instrument on IMAGE spacecraft is currently obtaining radio remote-sensing data about the density distribution of magnetospheric plasmas. The main RPI active sounding measurement is the plasmagram (Figures 1a and 1b) showing received signal strength (image intensity) as a function of echo delay (plotted as range along the vertical axis) and radio-sounder frequency (horizontal axis) of the radar pulses. Radar echoes from important magnetospheric structures, such as the magnetopause and the plasmapause, appear as traces on plasmagrams (thin black lines observed above 400 kHz in Figure 1a). Plasmagram traces are intermixed with vertical line signatures corresponding to the locally excited plasma resonances (e.g., intensification near 320 and 380 kHz in Figure 1a) and various natural emissions propagating in space.

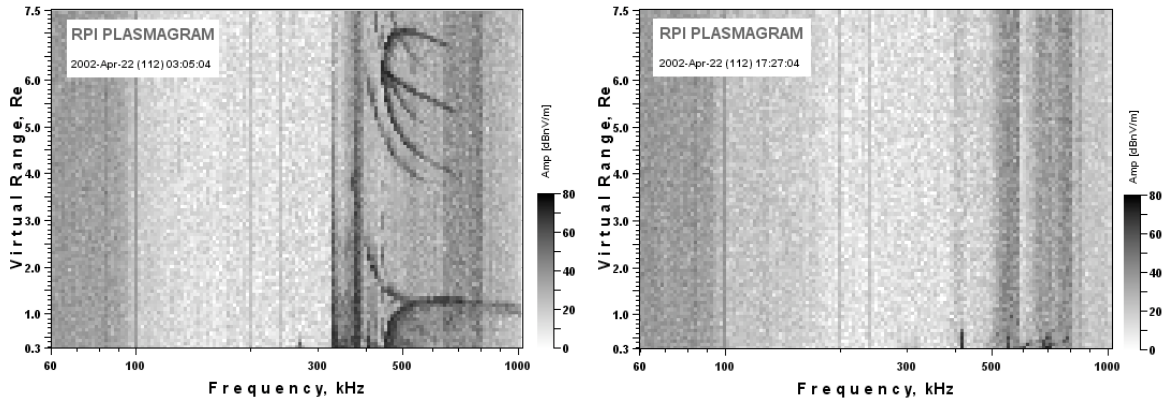

(a) Plasmagram with traces **(b) Plasmagram without traces**

Figure 1. (a) IMAGE RPI plasmagram recorded at 03:06:04 UT on April 22, 2002, showing signal reflections from remote plasma locations (dark traces) intermixed with stimulated resonances in the local plasma (vertical lines) and natural radio emissions (vertical bands). (b) 14 hours later, when the IMAGE spacecraft is located at a similar orbit position, remote reflections are not observed.

Less than 20% of all plasmagrams contain echo traces because RPI is a radar of opportunity: for its 10-Watt signal to reflect at a remote location as far as 40,000 km away, return to the spacecraft location, and appear above the noise level to be detected, a number of conditions needs to be satisfied. Figure 1b shows a plasmagram without visible traces of remote signal reflections. Although this measurement was taken during the same day at a similar orbit location, the required conditions for signal propagation were not met.

Manual search and processing of plasmagrams with traces is a major exercise requiring a significant amount of labor. Typically plasmagram scalers analyze 300-400 plasmagrams a day, which roughly translates to 12 years of non-stop work to process the available 1,200,000 images. We estimate that not more than 5% of all collected data will ever be looked at by human operators; an automated pre-classification shall improve chances that those 5% of data are useful.

4. PRE-ATENTIVE VISION: PREVIOUS WORK

Bottom-up perceptual grouping under restriction of the Gestalt's good continuation principle (Figure 2) is a natural choice for the task where top-down model considerations are lacking maturity because of the novelty of the RPI experiment. Figure 2(a) shows a synthesized pattern of *oriented edgels*, edge elements found by locating sharp intensity gradients in the image and evaluating their local orientation. Figure 2(b) shows edgel grouping results that identify 5 contours in the input pattern.

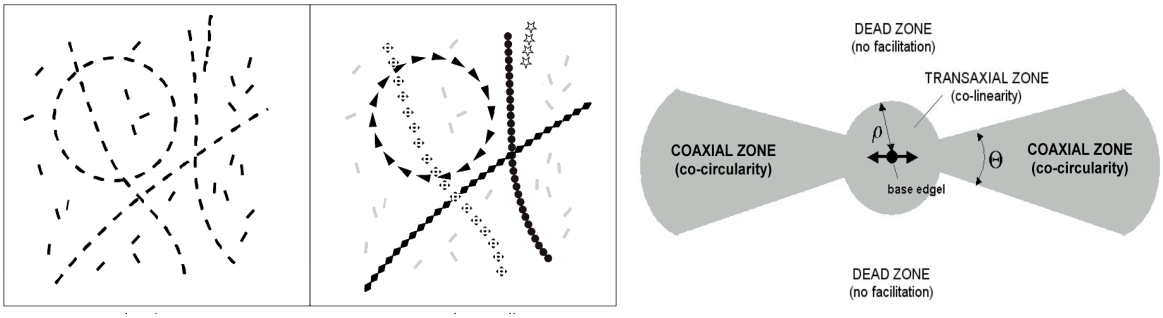

(a) Input edgels **(b) Grouping results** **(c) Zones of edgel interaction**

Figure 2. Perceptual grouping under restriction of the Gestalt principle of good continuation [4]-[11]. Input pattern (a) consists of oriented edge elements (edgels) found by a detector sensitive to intensity gradients in the image. Grouping results (b) show found salient contours. Grouping is governed by calculations of "saliency", a sum of weighted contributions from the neighboring edgels, depending on their mutual orientation, distance, and zone (c).

The grouping procedure is governed by calculations of the "saliency", first defined in [5] as a particular measure of length and smoothness of a contour. Biologically plausible models of saliency calculations [4], [6], [7] suggest that interaction between edgels depends on their mutual orientation and distance, and this dependence has different characteristics in three zones: coaxial, transaxial, and dead zone (Figure 2(c)). In the coaxial zone the saliency is highest for edgels that lie on the same arc (in agreement with the Gestalt's co-circularity [4]-[11]). Edgels outside the coaxial zone sectors do not contribute to the saliency measure, thus constituting two dead zones. Edgel interaction at close distances in the transaxial zone follows the principle of co-linearity instead of co-circularity (i.e., saliency is highest for edgels that are parallel to the base edgel). Summary contribution from all edgels within the gray area of the pattern in Figure 4 constitutes the likeliness for the base edgel to be a part of a contour.

After saliencies are calculated for all edgels in the image, the resulting saliency map is analyzed for presence of contours by a technique that is often referred to in the literature as "synchronization-desynchronization" [12] to reflect observed neural activity in the cortical networks of the brain. This task requires elements of attention-driven analysis if the image contains multiple features. Feature binding schemes [4] can replicate operations of attention switching and inhibition by introducing multiple layer models where separate features fall into different layers and thus become isolated from each other.

5. PRE-ATTENTIVE MODEL FOR PLASMAGRAMS

Replicating the plasmagram interpretation process is a difficult task. Only <1% of collected plasmagrams display distinct features as in Figure 1a. More frequently, traces are faint and sketchy, as in Figure 3a, and their automated extraction is not trivial.

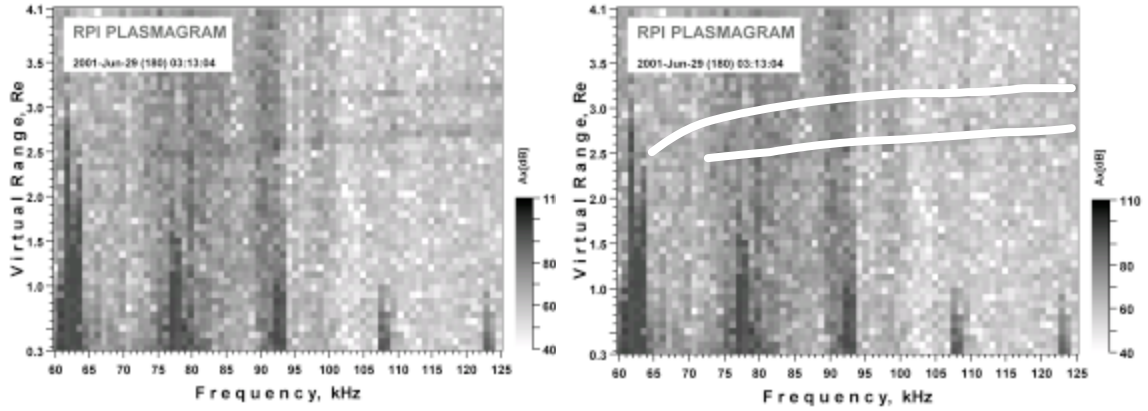

(a) Raw plasmagram **(b) Scaled traces**

Figure 3. Manual interpretation of an RPI plasmagram recorded at 03:13:04 UT on June 29, 2001, showing two faint traces of signal reflections at 2.5 and 3.0 R_E distance from the spacecraft. (a) Raw plasmagram, (b) manually scaled traces. Vertical lines correspond to stimulated plasma resonances.

There are additional challenges to consider. Real-life traces are thin lines (often just 1 pixel wide) immersed in a noisy, textured background. Image smoothing, a common protection of edgel detectors from noise, easily damages such thin traces. Without smoothing, not only edgel detector creates high number of false positives, but also it frequently mistakes position of true edgels and their orientation. Jitter of edgel position and orientation causes "washout" of calculated saliency of the contours. We also found that weak and short plasmagram traces are often indistinguishable in the saliency map because there are strong and long traces nearby.

A few improvements to the pre-attentive model were suggested previously [9] to help with plasmagram processing. Because locally evaluated orientations for edgels can be wrong for various real-life reasons, the decision is made to let them change their orientation under collective facilitation of edgels in a larger context area, because these local errors are only visible in a larger context. The oriented edgels are then called *rotors* to denote their ability to change orientation. Similar to other rotor models [10], [11], [13], the optimal orientations are found iteratively by means of a recurrent neural network that evolves into the global minimum of its energy.

Figure 4 illustrates calculations of synaptic weights for rotor interaction in co-linear and co-circular zones.

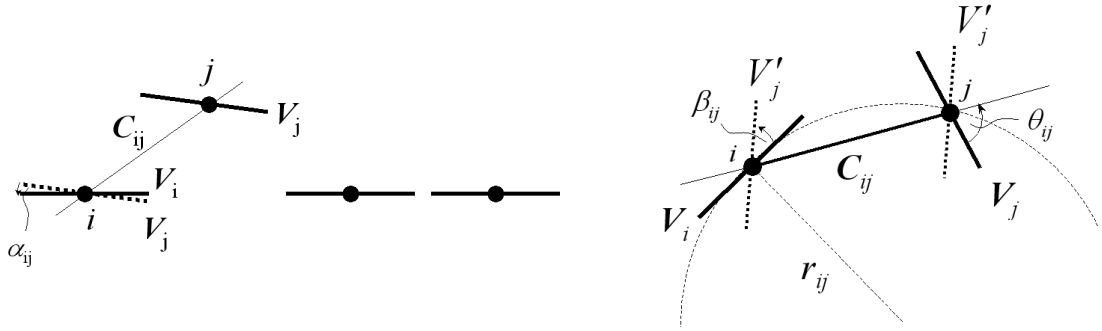

(a) Co-linear interaction in transaxial zone **(b) Co-circular interaction in co-axial zone**

Figure 4. Calculations of synaptic weights in the recurrent neural network. Use of co-linear interaction model in the transaxial zone improves robustness of saliency calculations to range jitter.

The neural network iteratively updates orientation and length of each rotor $\mathbf{V}_i$ using the following rule:

$$\mathbf{O}_i = \tanh\left(\frac{\sum_{all\ j} \mathbf{V}_i \cdot W_{ij} \mathbf{V}_j}{T}\right), \quad W_{ij} = \begin{cases} \dfrac{(\cos\alpha_{ij})^a}{|C_{ij}|^b}, & |C_{ij}| < \rho \\ \dfrac{(\cos\beta_{ij})^c}{|C_{ij}|^d} \begin{pmatrix} \cos 2\theta_{ij} & \sin 2\theta_{ij} \\ \sin 2\theta_{ij} & -\cos 2\theta_{ij} \end{pmatrix}, & |C_{ij}| > \rho \text{ and } |\theta_{ij}| < \Theta/2 \\ 0, & |C_{ij}| > \rho \text{ and } |\theta_{ij}| > \Theta/2 \end{cases}$$

where $\mathbf{O}_i$ is updated rotor $\mathbf{V}_i$ obtained by summing weighted contributions from other rotors $\mathbf{V}_j$ in the vicinity of $\mathbf{V}_i$. The sigmoid function *tanh* and temperature *T* are attributes of the recurrent feedback neural networks that use mean field theory formalism [13] and simulated annealing schemes in order to avoid local minima of energy and reach the global minimum. The synaptic weights W_{ij} implement perceptual grouping constraints using Gestalt constraints appropriate for three zones of interaction pattern shown in Figure 2(c). Zone boundaries are specified by ρ (radius of the transaxial zone) and Θ (central angle of the co-axial zone). α_{ij}, β_{ij}, and θ_{ij} are angles between rotors $\mathbf{V}_i$, $\mathbf{V}_j$, and connecting chord $\mathbf{C}_{ij}$ as shown in Figure 4.

The bio-plausible pattern for interaction of rotors appeared to be a valuable addition to the original rotor model [10]-[11]. Co-linear model for close range interaction in the transaxial zone helped to cope with the observed jitter of edgels positions, and addition of the dead zones improved analysis of weak traces in the presence of nearby strong traces. In summary, we combined two concepts, recurrent optimization of rotor orientation from Physics and pattern for rotor interaction from Biology to create our technique. Using this combination, we developed the Cognitive Online Rpi Plasmagram Ranking Algorithm (CORPRAL) [9] for prospecting the plasmagram archive.

6. PERFORMANCE TESTS

Figure 5 is a sample CORPRAL analysis of the plasmagram taken on March 01, 2002 00:02UT.

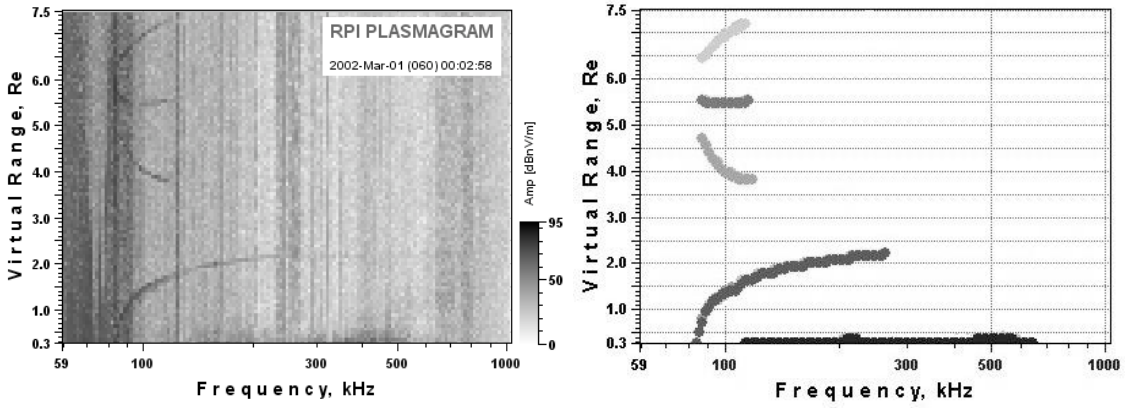

(a) (b)

Figure 5. CORPRAL plasmagram prospector detected 5 traces in RPI plasmagram recorded at 00:02:58 UT on March 01, 2002. (a) raw plasmagram, (b) automatically scaled traces.

All of available 1.2 million plasmagrams were processed to detect traces; over 200,000 of them are now labeled in the RPI mission database as containing echo signatures. We tested CORPRAL performance on a test set of 25,000 manually interpreted plasmagrams with 8% prevalence to obtain 94% overall accuracy of plasmagram prospecting and sensitivity of 85%. With prevalence below 10%, CORPRAL's positive predictive value drops to 50-60%, reflecting our choice to bias prospecting toward the false positive errors in order to increase its sensitivity to faint plasmagram traces.

7. DISCUSSION

With the suggested modifications, the pre-attentive vision model performed quite accurately as the RPI plasmagram prospector. However, errors in labeling plasmagrams (6% of the test dataset) continue to be our concern. False positive CORPRAL detections are most visible to human analysts working with the prospected data, and false negatives usually correspond to cases of weak and spread echoes (e.g., plasmagram in Figure 2a) that are of special interest to the RPI science team. We attribute most of the erroneous CORPRAL classifications to the early stages of image reduction to edge elements. In the pre-attentive, bottom-up approach these initial errors propagate up uncompensated, and only attention-driven verification of found signatures can remedy them. Edgel detection is not trivial when signal-to-noise ratio is low; our present and future work is concentrated on development of fast and reliable 1D and 2D algorithms for enhancement of weak and spread image features.

8. ACKNOWLEDGEMENTS

The work at the University of Massachusetts Lowell was supported by NASA under subcontract 83822 from Southwest Research Institute and through the Intelligent Systems (IS) Grant NNG04GO35G.

REFERENCES

[1] B. W. Reinisch, et al, "The Radio Plasma Imager investigation on the IMAGE spacecraft", Space Science Reviews, Vol. 91, 2000, pp. 319-35.

[2] J. L. Burch (ed), The IMAGE Mission. Dordrecht: Kluwer Acad. Pub., 2000.

[3] I. Rock and S. Palmer, "The legacy of Gestalt psychology", Scienific American, Vol. SCA9012, 1990, pp. 84-90.

[4] H. Wersing, J.J.Steil, and H. Ritter, "A competitive layer model for feature binding and sensory segmentation of features", Neural Computation, Vol. 13, 2001, pp. 357-387.

[5] A. Shashua and S. Ullman, "Structural saliency: the detection of globally salient structures using a locally connected network", 2nd International Conference on Computer Vision, 1998, pp. 321-327

[6] S.C.Yen and L.H. Finkel, "Extraction of perceptually salient contours by striate cortical networks", Vision Research, Vol. 38, 1998, pp. 719-741.

[7] G. Guy and G.Medoni, "Inferring global perceptual contours from local features", International Journal of Computer Vision, Vol. 20, 1996, pp. 113-133.

[8] P. Parent and S.W. Zacker, "Trace inference, curvature consistency, and curve detection", IEEE Transactions, Vol. PAMI-11, 1989, pp 823-839.

[9] I. A. Galkin, B.W. Reinisch, G. Grinstein, G. Khmyrov, A. Kozlov, and S. F. Fung, "Automated exploration of the Radio Plasma Imager data", Journal of Geophysical Research, Vol. 109, 2004.

[10] S. Baginyan, A. Glazov, I. Kisel, E. Konotopskaya, V. Neskoromnyi, and G. Ososkov "Tracking by a modified rotor model of neural network", Computer Physics Communications, Vol. 79, 1994, pp. 165-178.

[11] I.A. Galkin, B.W. Reinisch, G.A. Ososkov, E.G. Zaznobina, and S.P. Neshyba, "Feedback neural networks for ARTIST ionogram processing", Radio Science, Vol. 31, 1996, pp. 1119-1129.

[12] Yen, S.C., E.D. Menschik, and L.H. Finkel, "Perceptual grouping in striate cortical networks mediated by synchronization and desynchronization", Neurocomputing, Vol. 26-27, 1999, pp. 609-616.

[13] C. Peterson, "Track finding with neural networks", Nuclear Instruments and Methods in Physics Research, Vol. A279, 1989, pp.537-545.